

ORIGINAL RESEARCH

Deep learning model for enhanced power loss prediction in the frequency domain for magnetic materials

Dixant Bikal Sapkota  | Puskar Neupane  | Mecon Joshi  | Shahabuddin Khan

Department of Electrical Engineering, Pulchowk Campus, Tribhuvan University, Lalitpur, Nepal

Correspondence

Dixant Bikal Sapkota, Department of Electrical Engineering, Pulchowk Campus, Tribhuvan University, Lalitpur, Nepal.
Email: dixantbs7@gmail.com

Abstract

This paper outlines the methodology for predicting power loss in magnetic materials. It starts by introducing the concept of core loss and the complexity of modelling it. Steinmetz's equation is presented to calculate power loss based on frequency and magnetic flux density, but its limitations are highlighted. As an alternative, a neural network-based method is introduced. The proposed methodology adopts a long short-term memory network, expressing the core loss as a function of magnetic flux density, frequency, temperature, and wave classification. Fast Fourier transform was implemented to reduce the data points of the sampled flux density waveform while preserving its characteristics. Analyzing in the frequency domain enabled streamlining the training of the model. The input features were arranged as required, and the network architecture was designed with appropriate layers and optimal activation functions. Through extensive training using the datasets, the model assimilated intricate relationships between input variables and known power loss. Evaluation and validation metrics were subsequently employed to gauge the performance of the trained network. This innovative methodology aims to significantly augment the precision of power loss predictions, providing valuable insights into the nuanced behaviour of magnetic materials.

1 | INTRODUCTION

Magnetic materials are typically characterized by their magnetic domain existence. In the absence of an external magnetizing field (H), these domains are aligned randomly. However, in the presence of such a field, these domains tend to adjust themselves to align in parallel with the direction of the applied field. In a condition where an alternating current is applied, the direction and magnitude of the external field keep alternating periodically. Due to this, the alignment of the domain oscillates with the frequency of the applied field. This repeated action of change in direction and magnitude of the domain generates heat in the body, causing a part of the phenomenon known as core loss. In the case of conductive materials core loss also includes the loss from eddy currents induced in the material.

Charles Steinmetz first developed the equation to characterize the magnetic core loss in 1892. It is an empirical formula that is used to compute the overall losses of power in any magnetic material expressed as power loss per unit volume. It was

later modified to include frequency term and named Steinmetz's equation [1]. The equation is mathematically expressed as:

$$P_v = k f^a B^b \quad (1)$$

Here, P_v is the average power loss per unit volume, f is the frequency, B is the peak value of magnetic flux density and k , a , and b are Steinmetz constants whose values are obtained through the B - H curve fitting of a given material. This equation gives a simple understanding of core losses, that the power loss scales with frequency and magnetic flux density. It is a decent equation for the general design of equipment whose power losses are not too large. However, the assumption of a power-law relationship between core loss and frequency, may or may not hold for different materials and frequency ranges. Also, at much higher frequencies, the skin effect and proximity effect become very significant which is not accounted for in this equation. Moreover, this equation does not consider the geometry of the core, which can be crucial in determining losses. On top of all these

flaws, the equation assumes an idealized magnetic circuit, which does not capture the complexities of real-world machines.

It is known that when designing inductive components, core loss calculations can be difficult problems to solve. [2] has stated that the Steinmetz equation is only applicable for sinusoidal excitation which has become its major drawback because most power electronic devices are exposed to non-sinusoidal flux waveforms. In the field of power electronics, this equation is perhaps the weakest link due to its ignorance of the impact of various other factors on power losses, which include—the impact of waveform shape, the impact of DC bias in the magnetizing field, the impact of ambient and core temperatures and more.

Over the years following, various models were developed to overcome the shortcomings of the Steinmetz equation (SE). For instance, Modified SE (MSE) [3, 4] and generalized SE (GSE) [5] improved the results under non-sinusoidal excitation. Further, the improved generalized SE (iGSE) was developed, which has been considered a very good method for calculation. According to [6] it is expressed as:

$$P_v = \frac{1}{T} \int_0^T k_i \left| \frac{dB}{dt} \right|^a (\Delta B^{b-a}) dt \quad (2)$$

Where, ΔB represents the flux density from peak to peak and k_i is given by:

$$k_i = \frac{k}{(2\pi)^{a-1} \int_0^{2\pi} |\cos\theta|^a 2^{b-a} d\theta} \quad (3)$$

This equation is capable of computing the losses with almost any waveform shape while using the same parameters as the original equation. However, it gives large errors for very high or very low duty cycles [7]. Furthermore, [8] states that despite Steinmetz equation and its extension, iGSE, being relatively accurate models for calculating core losses in general cases, some core-loss phenomena cannot be well described with an equation consisting of only three overall parameters.

Similarly, according to [7] methods such as equivalent elliptical loop (EEL) and waveform coefficient SE (WcSE) give high errors when the duty cycle is far from 0.5. Other methods such as double natural SE (DNSE), improved-iGSE (i²GSE), rectangular extension of SE (RESE) and, filtered-improved generalized SE (FGSE) introduce new parameters which are not typically available in the data sheets [7].

Magnetic components play a key role in power electronic converters, however, modelling these components is still a challenge today. The above-discussed equation-based techniques are computationally costly, dependent on certain material characteristics, and frequently require large-scale observations [9]. Being able to accurately predict the core losses of magnetic materials would immensely help in designing higher-performance magnetics.

In recent times, models based on neural networks have been considered for magnetic core loss prediction due to their

effectiveness in solving non-linear problems. These models are data-based in nature and can predict losses for a given material subjected to a certain field density with known frequency, temperature and, any appropriate additional features. This approach requires careful study of impacting parameters, design of an appropriate model architecture, large and accurate data set coupled with an optimal training process. The nonlinear relationship of magnetic core losses with various parameters like frequency, flux density and temperature can be appropriately captured by deep neural networks (DNNs). Alongside this, various model architectures can be developed for different materials with similar or dissimilar properties. DNN models can learn from datasets that include real-world variability and account for factors that may not be considered in simplified empirical equations, like the Steinmetz equation.

This is the approach taken in this paper. Leveraging the power of the Python programming language and a large number of available libraries such as *numpy*, *pandas*, *tensorflow*, and *keras*, a model has been designed with capability of predicting losses for any magnetic material with a good accuracy and relatively small number of input features.

2 | LITERATURE REVIEW

Within this specific field, prior research and parallel efforts have paved the way in a similar context. Crucial datasets necessary for training, validation, and testing of the model have been obtained from earlier works [10–12], significantly contributing to the preparatory phases of this study. These datasets, derived from previous investigations, assume a pivotal role in refining and evaluating the model.

It has always been a challenge to predict the core losses in the design of devices such as inductors, transformers, and various other electric machines. Paper [13] proposes a dynamic model to estimate and predict losses in ferromagnetic and ferrite materials with arbitrary flux waveforms. The alternative time domain model is based on the idea of elliptical loop equivalence. The authors claim the model to be practical for industrial applications as it provides reasonable accuracy and uses actively available data for prediction.

The estimation of core loss with a limited dataset and the establishment of connections between input and output parameters present a substantial challenge. The integration of deep learning methodologies has facilitated the acquisition of intricate relationships and nuanced features within the dataset [14]. Leveraging back-propagation for the adjustment of internal parameters has improved the learning behaviour, particularly through the incorporation of multiple layers. Recurrent neural network (RNN) has demonstrated significance in time series prediction, wherein the utilization of data from preceding predictions or processes contributes to the subsequent prediction state [15]. The authors in [16] have presented a computer-generated core loss electron energy loss spectroscopy (EELS) dataset which is useful for training various neural networks. The previous methods of automated identification

of core-loss edges had very little success due to high noise sensitivity. Multiple neural network structures have been optimized and then evaluated in terms of accuracy and efficiency.

Conversely, long short-term memory (LSTM) which is a sub-type of RNN [17], has shown its value in addressing nonlinear tasks by capturing and retaining relevant information across extended sequences [18]. This is attributed to the architectural inclusion of memory cells and gating units, allowing selective recall or forgetting of information. LSTM networks prove advantageous in tasks demanding the modelling of complex temporal dependencies, particularly enhancing performance in scenarios necessitating the resolution of time-lag issues over prolonged duration in sequences or time-series data. This capability proves particularly beneficial in maintaining context even in instances of significant time lags, often exceeding 1000 steps [19].

A comprehensive survey conducted in [20] explores various publications delving into the application of artificial intelligence in power electronics. This article comprehensively reviews AI methods in power electronic systems, categorizing them by application, method, and function. It identifies key findings, such as the categorization of AI methods into design, control, and maintenance. The objective is to enhance accuracy and efficiency within the sector, thus highlighting the potential of AI methodologies in power electronics applications. The article emphasizes that AI applications primarily deal with optimization, classification, regression, and data structure exploration.

The advancement of various machine learning algorithms, along with their extensive applications, has rendered them suitable for predicting magnetic core losses. Several studies have already employed these machine learning algorithms and tools, demonstrating their superior accuracy compared to earlier methods of loss calculation by equation and formula. This type of machine learning algorithm is not limited to a particular field but is valuable to every sector as the deep learning methods have achieved good results in the field of power fingerprint identification, such as CNN, RNN etc. [21]. The data sheets for loss and B - H loop utilizing neural networks are presented in [22], along with an illustration of how neural networks are useful for core loss predictions. With a neural network, the magnetic core loss of various materials may be more accurately predicted under various operating conditions. The deep neural network (DNN) method was implemented in [23], which accurately modelled the core losses and recommended capturing additional scenarios to enhance the model. The most advanced neural network models have also been put into practice, and they have shown to be more accurate in predicting core losses than traditional machine learning models. The transformer neural network model described in [24] has proven to be effective in simulating hysteresis loops by symbolically integrating sequence inputs and scalar inputs.

Efficiency mapping has an important role in determining the efficiency distribution and the energy consumption of electric motors. Performing this analysis at all different operating points with finite element method (FEM) analysis

during the designing process requires intense processing capabilities. In [25] a machine learning-based model was developed to overcome the extensive processing required during FEM analysis.

Transfer learning is a popular machine learning technique that makes use of pre-existing models to create new models with minimal resources. The exploration conducted in [26] focuses on experimenting with two specific transfer learning approaches: material-to-material transfer learning and waveform-to-waveform transfer learning. The study attests to the efficacy of these transfer learning techniques, demonstrating how they may be used to leverage expertise from one domain to improve performance in another.

The authors of [27] present a deep neural network (DNN) based approach to predict core losses in magnetic materials. The paper also compares different DNN structures and develops a new DNN model based on experimental data. The proposed structure is envisioned to be implemented for loss estimation for electrical machine design and optimization, as it can provide robust and accurate predictions. Similarly, [28] presents a method for predicting the specific power loss in ferromagnetic cores using LSTM-GAN (generative adversarial network).

An accurate field solution is required for the analysis of electromagnetic (EM) devices such as transformers and other electrical machines, into which decades of research and development have gone, for fast design analysis. [29] has studied and investigated the feasibility of Deep learning algorithms to predict solutions of Maxwell's equations in low-frequency electromagnetic equipment. The presented model has efficiently enabled the authors to generate the field distribution for various geometries and shapes at a lower computational cost.

3 | FOURIER TRANSFORM AND FFT

Fourier transform [30] is a mathematical technique that decomposes any signal which is a function of time into its various constituent frequency components. In simple words, it takes any signal and represents it in terms of the frequencies that make it up. This is a transformation between time-domain representation and frequency-domain representation. Mathematically, a continuous Fourier Transform of any function $f(t)$ is given as:

$$F(w) = \int_{-\infty}^{\infty} f(t) \cdot e^{-jw t} dt \quad (4)$$

Here, $F(w)$ is the frequency domain representation of the given function and w is the frequency, $f(t)$ is the original function, and $e^{-jw t}$ represents a complex exponential function.

Fast Fourier transform, abbreviated as FFT, is a mathematical algorithm that computes the discrete Fourier transform. [31] The “numpy” library in Python provides functionality for calculating one-dimensional n -point discrete Fourier transform with the FFT algorithm. The input to the FFT algorithm is an array of sequential data points representing a sampled time series data

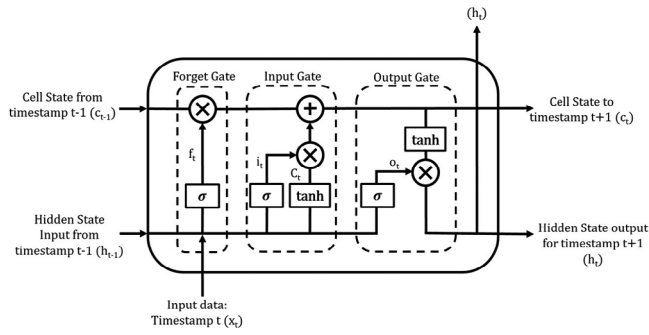


FIGURE 1 Single LSTM cell with forget, input, and output gate [32].

and its result is an array of complex numbers representing the samples of frequency domain spectrum. Only the first half of the output array is to be considered, as the maximum frequency that can be represented in the time domain is half of the sampling frequency. The fast Fourier transform (FFT) has been used in reducing the computational complexity of the model by reducing the input parameters required for calculation.

4 | LSTM

The LSTM model is a kind of recurrent neural network that effectively transfers information between steps to solve the vanishing gradient problem. A singular LSTM cell, as seen in Figure 1, comprises three fundamental components: the input gate, output gate, and forget gate. The equation for these gates in LSTM is represented by expressions 5, 6, and 8.

$$f_t = \sigma(W_f * [b_{t-1}, x_t] + b_f) \quad (5)$$

$$i_t = \sigma(W_i * [b_{t-1}, x_t] + b_i) \quad (6)$$

$$o_t = \sigma(W_o * [b_{t-1}, x_t] + b_o) \quad (7)$$

$$c_t = c_{t-1} * f_t + i_t * C_t \quad (8)$$

The input, forget, and output gates in long short-term memory (LSTMs) combine to produce an intricate gating mechanism that is essential for solving the vanishing gradient problem and identifying long-term dependencies in sequential data. The forget gate controls the recall of prior knowledge, the output gate controls the ultimate output, and the input gate controls the relevance of incoming information. LSTMs can selectively process information thanks to this complex gating structure, which helps them overcome limitations in conventional recurrent neural networks. Because LSTMs are so good at identifying complex patterns in sequential data, they are particularly well-suited for tasks involving time series or natural language processing, where strong learning requires the capture of extended relationships.

TABLE 1 Material information.

S.N	Materials	Curie temp	μ_i	Resistivity
1.	3C90	>220 °C	2300 \pm 20%	5 Ω m
2.	3C94	>220 °C	2300 \pm 20%	5 Ω m
3.	3E6	>130 °C	12,000 \pm 20%	0.1 Ω m
4.	3F4	>220 °C	900 \pm 20%	10 Ω m
5.	77	>200 °C	2000	1 Ω m
6.	78	>200 °C	2300	2 Ω m
7.	N27	>220 °C	2000 \pm 25%	3 Ω m
8.	N30	>130 °C	4300 \pm 25%	0.5 Ω m
9.	N49	>240 °C	1500 \pm 25%	17 Ω m
10.	N87	>210 °C	2200 \pm 25%	10 Ω m

5 | MATERIAL INFORMATION

A total of 10 different magnetic materials were used in this paper to create a model to accurately predict their core losses. **3C90** is a low-frequency power material used in transformers up to around 0.2 MHz of frequency. Similarly, **3C94** is also used in transformers but up to around 0.3 MHz of frequency. **3E6** is a high permeability material that is optimized for use in wide-band transformers as well as EMI-suppression filters. **3F4** is a high frequency power material for use in transformers at frequencies range of 1–2 MHz. **77** is a ferrite used in a variety of high and low flux inductor designs for frequencies up to 100 KHz. **78** is also a ferrite designed for power applications for frequencies up to 200 KHz. **N27** and **N49** are preferably used in power transformers. **N30** is used in broadband transformers. **N87** forms an essential part of inductors and transformers that are used in various application areas of power conversion, communications, and suppression of interference. Table 1 contains some specific parameters relating to each of the materials, collected through various data-sheets.

Here, initial permeability (μ_i) is recorded for a temperature of 25 °C and frequency less than 10 KHz. Also, the resistivity is recorded under DC conditions at 25 °C.

6 | METHODOLOGY

6.1 | Data collection

Data for training, validation, and testing of the deep learning algorithm were sourced from references [10]–[12] as part of the MagNet Challenge 2023.

6.2 | Data processing

The datasets encompassed information for 10 materials, each comprising five distinct comma-separated values (CSV) files. These files provided details on magnetic field density (B), applied magnetizing field force (H), frequency (F), temperature

TABLE 2 Total provided data for each of the materials.

Material	Instances/rows of training data
3C90	40,713
3C94	40,068
3E6	6996
3F4	6564
77	11,444
78	11,380
N27	11,396
N30	8978
N49	8602
N87	40,616

(T), and measured volumetric loss (V). For B and H waveform data, the CSV file contained 1024 time series points over a single cycle. The materials' names and the total data points (instances or number of rows) for the training dataset are presented in Table 2. An additional 5000 instances of data for each material were provided later as a validation set to test the trained model.

To reduce the computational time for training the models, there was a need to minimize the data size while preserving as much valuable information as possible to sustain accuracy. To achieve this, the focus was primarily set on the aggregation of the given waveform data. Various methods were explored, including selecting only a few of the numerous provided time instance values, averaging the values over a specific range, and decomposing the wave into its constituent harmonics but the latter seemed to give the most favourable results with higher consistency.

Fast Fourier transform, shortened as FFT, was employed to transform each of the provided time domain waveforms into its frequency domain representation. Specifically, the DC offset and the next 31 harmonics (i.e. first 32 terms in total) were used for model training. This technique preserved the wave characteristics during the training while also reducing the overall data input directly to the model. Since the output of FFT is a complex quantity, its absolute value was considered for each harmonic. This was done because if both real and imaginary values were to be used for model training, there would be twice as much data, which would increase the computational needs. The model's accuracy was observed to be largely unaffected by the inclusion of more harmonics; so, the terms were restricted to 32.

Additionally, further techniques were integrated to efficiently recognize and classify various waveforms. The waves were categorized into sinusoidal, triangular, and trapezoidal waves based on their frequency domain representations. Sine waves have high fundamental components and negligible harmonics thereafter, while triangular waves have a low fundamental component to second harmonic ratio and trapezoidal waves have a high value of the same ratio. These properties were used for the classification and it seemed to give an acceptable classification although there were some outliers in the trapezoidal and

triangular categories. Practically, sinusoidal waves were isolated first, and then waves having a fundamental component to the second harmonic component ratio of less than 7 were classified as triangular while more than that were classified as trapezoidal. An example of this can be seen in Figure 2.

The goal was to establish a cost-effective equilibrium between model accuracy and resource efficiency through the reduction of input data size and the proper classification of waveforms.

To fully understand the nature of the parameters for each material, various plots were drawn. A scatter plot drawn between different features for 3C90 can be seen in Figure 3. It can be observed that the data doesn't have any defined correlation. High volumetric losses exist for lower B_{\max} , but even at higher fields volumetric loss ranges significantly due to changes in frequency and temperature values. From Figure 3(d) it can be observed that high frequencies are only present for lower field densities. This is proved by the correlation between B_{\max} and frequency being -0.430108 . The effect of this can be observed in Figure 3(b) where, as we proceed to higher frequencies, the overall volumetric losses slightly decrease. Using `pandas.DataFrame.corr()`, the correlation between B_{\max} and volumetric loss was found to be 0.759792 . In the frequency domain, Figure 4 shows the correlation between various harmonics and loss. Here, B2 represents the fundamental or first harmonic, B3 represents the second harmonic, and so on. It can be seen that different harmonics have different correlations with loss. From Figure 4(a) it can be seen that the 1st, 9th, 11th, 19th, 21st, 29th, and 31st harmonics seem to have a much higher level of correlation and this pattern continues in a descending gradient as seen in Figure 4(b). Also, the 5th, 15th, and 25th harmonics seem to have a below-normal correlation with their corresponding power loss.

6.3 | Model architecture

The neural network model is a multi-input architecture, strategically tailored to address a specific task. There are four different input layers in the model, and each has a specific function. The first input layer is capable of processing data sequences having a particular shape of (32, 1) since it is set up to handle the waveform information. This arrangement corresponds to the expectation of input sequences with a length of 32. The following input layers support temperature and frequency numerical values in addition to a classification variable which is a categorization value that reflects the inherent characteristics of the applied waveform. An examination of the harmonic magnitudes served as the foundation for this conclusion. All of these input parameters are normalized.

To extract any temporal dependencies in the frequency domain, two long short-term memory (LSTM) layers with 128 units each were employed as seen in Figure 5. These LSTM layers play a pivotal role in capturing intricate patterns within the input. To augment the stability of the training process, batch normalization, and dropout mechanisms are incorporated between these two LSTM layers.

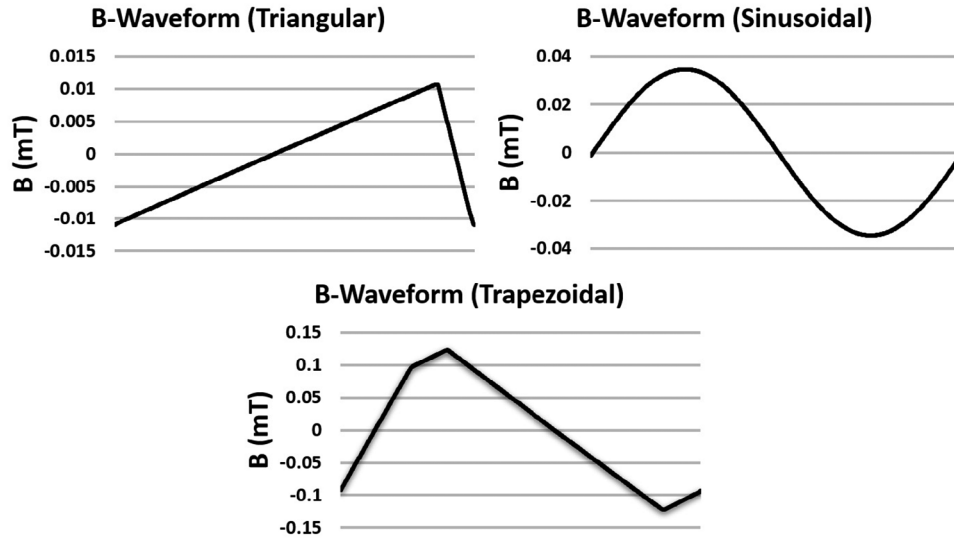


FIGURE 2 Classification of magnetic field density waveforms: triangular, sinusoidal, and trapezoidal.

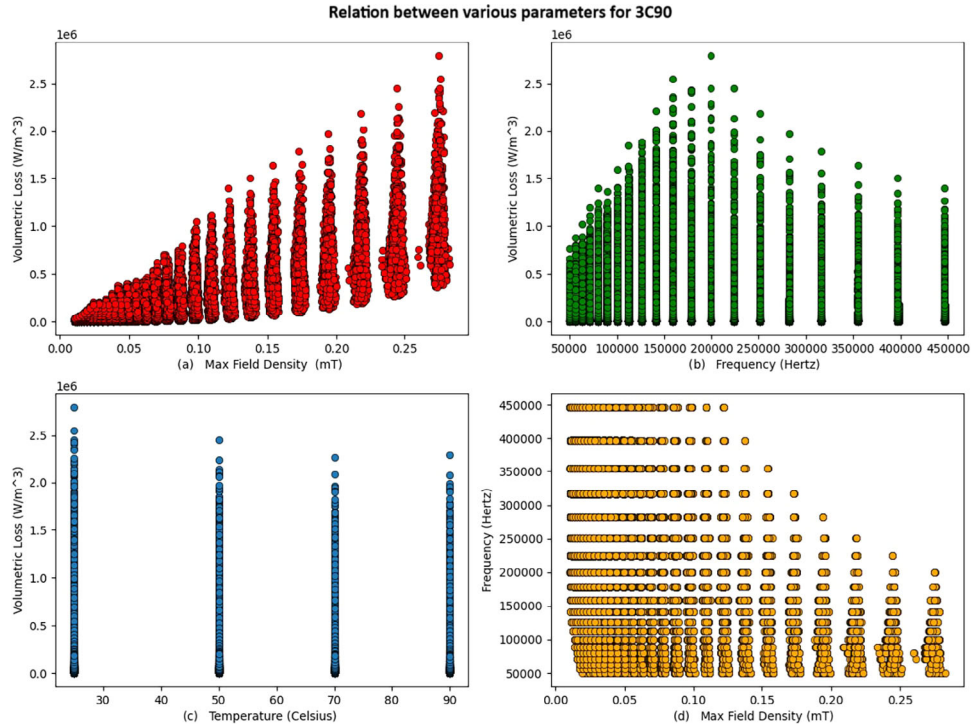


FIGURE 3 Scatter plot between various parameters for Material 3C90: a) maximum field density vs volumetric loss, b) frequency vs volumetric loss, c) temperature vs volumetric loss, d) maximum field density vs frequency.

The output features obtained from the LSTM layers are subsequently concatenated with the remaining inputs which are frequency, temperature, and classification. This consolidated input is then fed into the subsequent layers of the neural network. The processing of this concatenated input is executed through several dense layers, each equipped with rectified linear units (ReLU) as activation functions. ReLU activation is a piece-wise linear function which is given as:

$$f(x) = \max\{0, x\} \quad (9)$$

which signifies that the node gets activated only if the sum of weighted inputs is greater than 0, else, the node is deactivated, i.e. turned off. ReLU is used here because of its simplicity, general use case, and for reduction of vanishing gradient. The information on each of the dense layers is tabulated in Table 3.

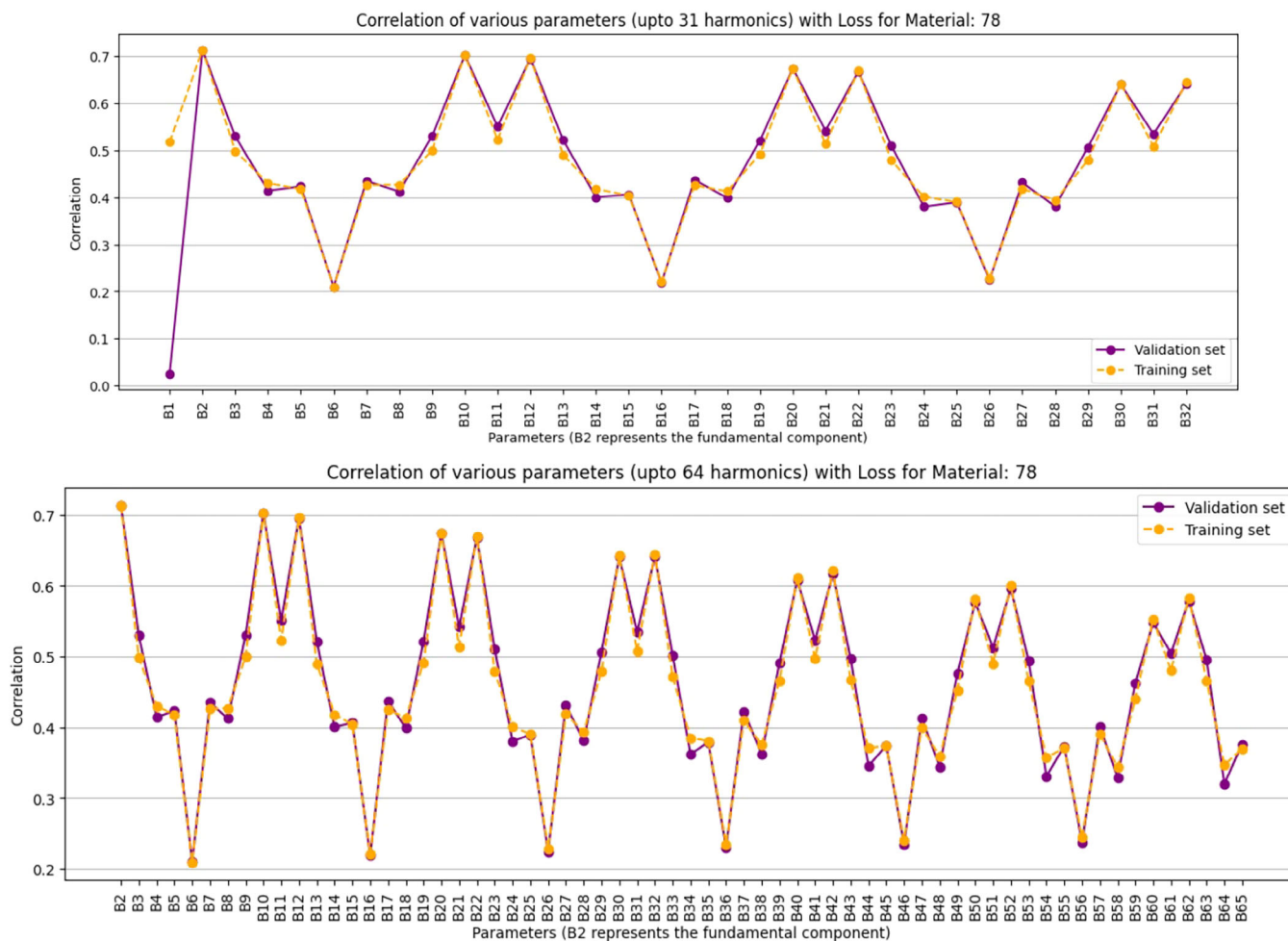


FIGURE 4 Correlation plot of loss vs various parameters for material 78 with (a) 31 harmonics and (b) 64 harmonics.

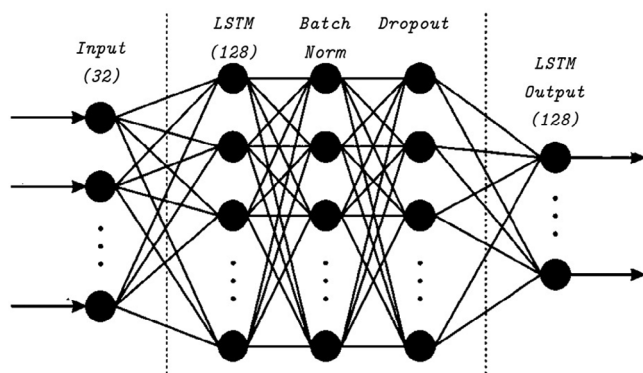


FIGURE 5 LSTM layer diagram.

Using the Adam optimizer, the model optimizes its parameters. The model's last layer, which produces a single-unit output layer, demonstrates adaptability for tasks involving regression or binary classification. Because of its design, the model may be made to adapt to a wide range of analytical circumstances, providing a thorough and reliable solution for the intended purpose. Table 4 lists all the details regarding the model

TABLE 3 Dense layer information.

Layer	Type	Neurons	Connected to
A	Dense	256	LSTM out
B	Dense	128	A
C	Dense	64	B
D	Dense	32	C
E	Dense	16	D
Output	Dense	1	E

parameters and size. The flowchart showing the sequence of data-preprocessing, arrangement of the new data sets and model layering can be seen in Figure 6.

6.4 | Training

Each model was trained for over 500 epochs. During training, *ModelCheckpoint* under *keras.callbacks* saves the model after a complete epoch if, at that point, it has a lower value of *validation loss*. Training time for each epoch ranges from 5 to 20 seconds,

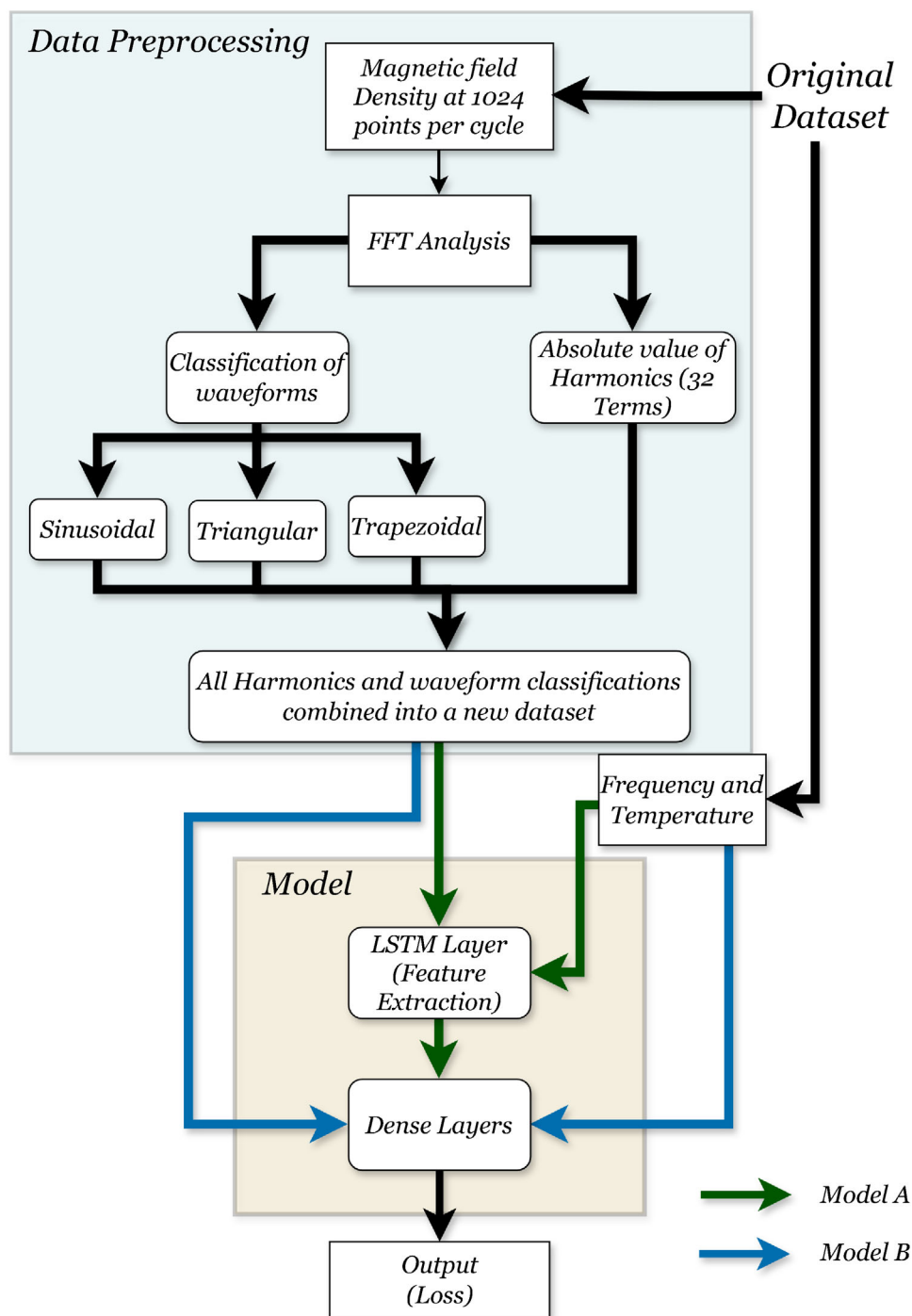


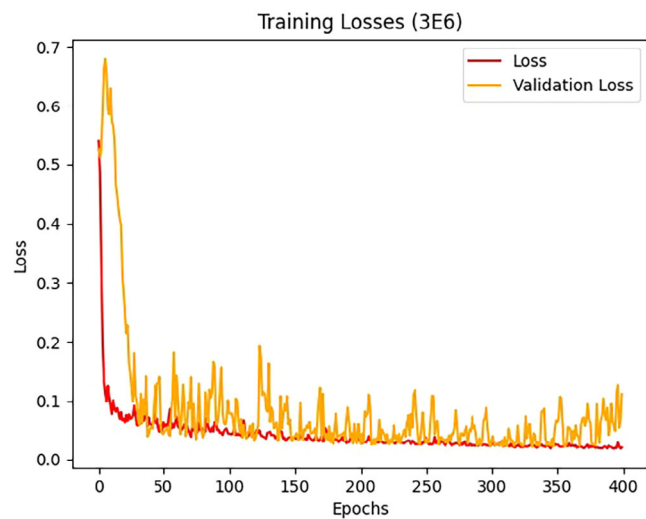
FIGURE 6 Flowchart showing the entire process.

varying based on batch size and training data size. The plot of training and validation losses, as seen in Figure 7 for material 3E6, shows that the model learns at a very high rate within the first few epochs, and gradually saturates over time. The noisy nature of validation loss is due to a smaller batch size during training. A smaller batch size allows the model to learn from each example of the training set but takes a longer time to train.

Initially, the model 'A' was trained for each material and was validated using the validation set. The model performed well, after several iterations of hyper-tuning, for most of the materials but had higher errors for some. Assuming the higher losses due to over-fitting of data, the complexity of the model was reduced for these materials. In doing so, it was found that model 'B', with a bypassed LSTM layer, performed slightly better.

TABLE 4 Model information.

Model	Info	Value
A (LSTM+dense)	Total parameters	276,225
	Trainable parameters	275,969
	Non-trainable parameters	256
	Size of file	1.05 MB
B (Dense)	Total parameters	193,537
	Trainable parameters	193,537
	Non-trainable parameters	0
	Size of file	0.756 MB

**FIGURE 7** Training and validation loss for material: 3E6.

7 | RESULTS

After training the model using the provided training data-set for each of the 10 different materials, each model's validity was individually tested using separate validation data sets, each consisting of 5000 data. To analyse the performance of the models, histograms were plotted with percentage relative error as the x -axis and ratio of data points as the y -axis, using *matplotlib*. The plot highlights and labels the overall average error, 95 percentile error, and the maximum error. The error distribution histogram was plotted for all of the ten materials.

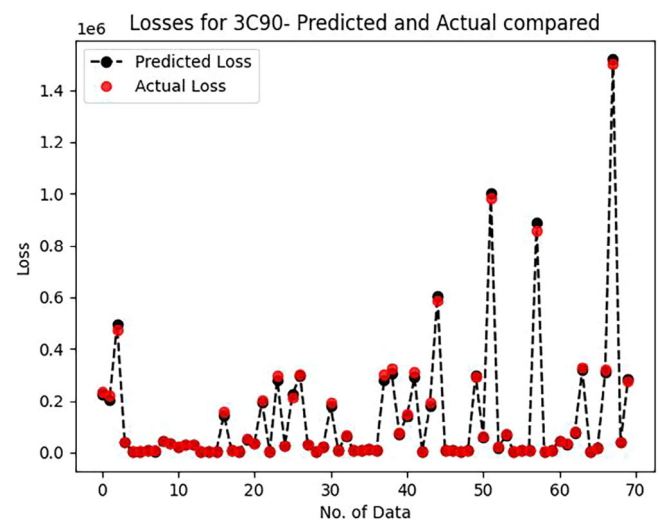
The performance of the model for each material can be observed in the histograms as seen in Figure 9. The losses for each material are also tabulated in Table 5. Error for each instance is calculated using Equation (10)

$$\text{Error(\%)} = \frac{|\text{meas} - \text{pred}|}{\text{meas}} * 100\% \quad (10)$$

Here, meas represents the measured loss provided in the dataset, and pred represents the prediction of loss from the model output. The predictions were outputted in a new list whose values range within the scaling limits. These values

TABLE 5 Average error and 95th percentile error for each material.

S.N	Materials	Average error	95th Prct. error	Model
1.	3C90	4.75 %	10.58 %	A
2.	3C94	4.30 %	12.10 %	A
3.	3E6	3.44 %	8.54%	A
4.	3F4	5.22 %	18.44 %	A
5.	77	6.15 %	17.66 %	A
6.	78	6.68 %	22.17 %	A
7.	N27	2.77 %	9.39 %	B
8.	N30	4.02 %	8.35 %	A
9.	N49	3.03 %	11.47%	B
10.	N87	4.53 %	15.50 %	A

**FIGURE 8** Actual losses vs predicted losses for material 3C90 for 70 random data points.

were all transformed back using *inverse_scaler* to their original range before the error was calculated. Figure 8 shows the plot between actual loss and predicted loss for the material 3C90.

7.1 | Comparative analysis

The works done in [11] and [12] have used LSTM and Transformer based models to predict the core losses for N87 using a $B-H$ loop prediction, using a similar but much larger dataset (142,871 data points). The comparative results are tabulated in Table 6. We can observe that, while the Transformer model performs better, the average error for both LSTM models is similar even though the training set size disparity is very large. This reflects that with adequate data, the frequency-domain approach for data preprocessing to reduce input parameters and classify waveforms is viable.

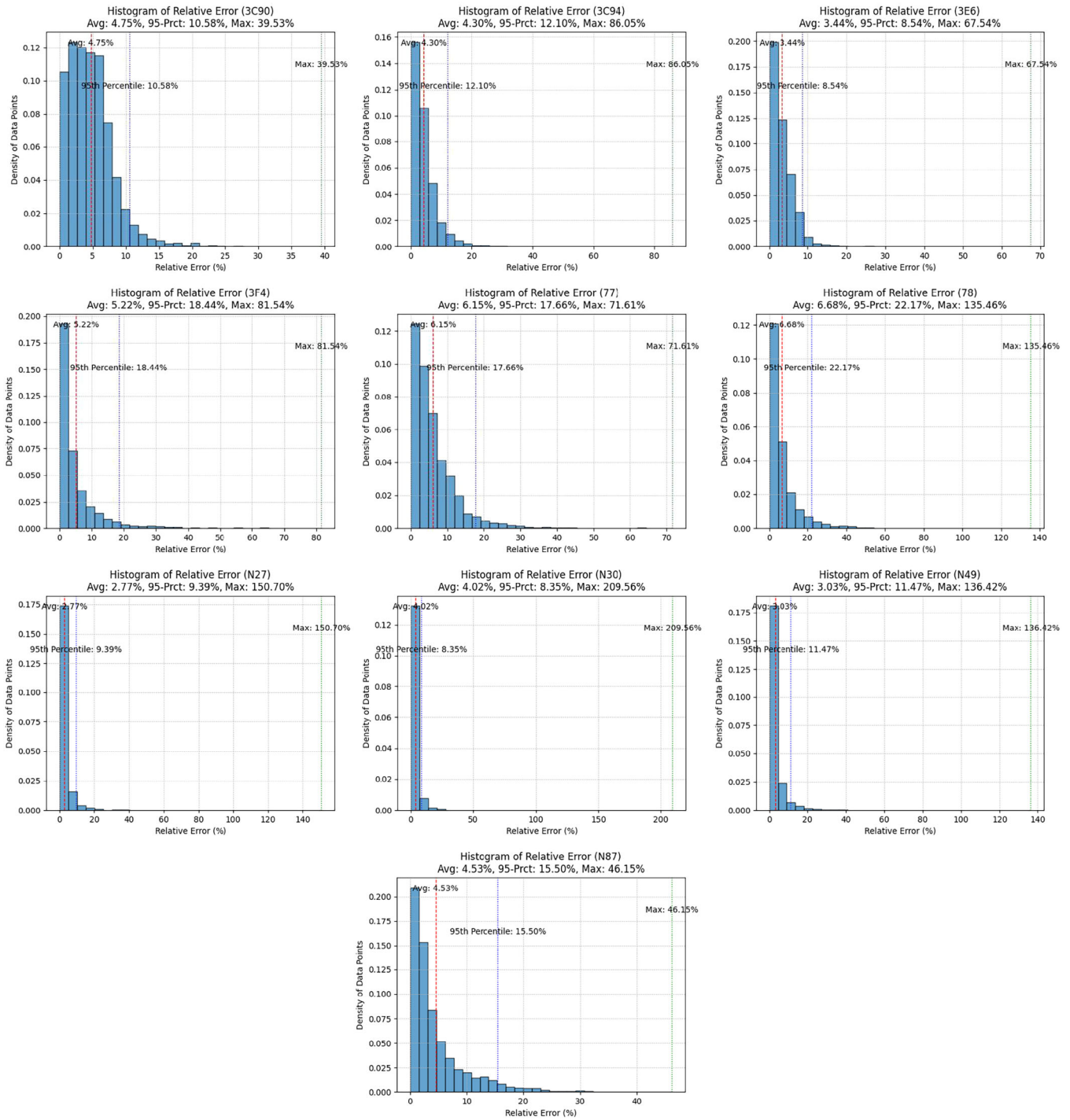


FIGURE 9 Error histogram depicting variations across 10 different materials showcasing average error, 95th percentile error, and maximum errors.

8 | CONCLUSIONS

In conclusion, this research presents a data-based approach to predict magnetic core loss. It acknowledges the importance of the use of conventional Steinmetz's equation and suggests a neural-network-based method to overcome some of its drawbacks. The datasets for training the model have been sourced from the MagNet challenge database for ten different materials.

To reduce the training complexity, the waveforms are analysed in the frequency domain by decomposition into harmonics, instead of the time domain which helped in the reduction of total features fed into the network. Also, the Fourier transform is used to analyse the nature of the waveforms and classify them, as part of pre-training data processing.

The designed neural network consists of several LSTM layers for feature extraction followed by dense layers with ReLU

TABLE 6 N87 error comparison with the results presented in [12].

N87	[12] results (142,871 data points)	Our results (40,616 data points)
Model:	LSTM	Frequency domain LSTM
Avg error (%)	4.517%	4.53%
95-Prct error (%)	10.9%	15.5%

activation and an adjustable output layer. The accuracy of this model has been demonstrated via the histograms that indicate the percentage relative error of the results. The average error is less than 7% and the 95th percentile error is less than 23% for all the ten materials considered.

The usefulness of this methodology in improving power loss forecasts for various materials and operating conditions has been emphasized in the paper. Empirical and analytical approaches cannot yield accurate estimates for all circumstances whereas our data-driven model can do so by uncovering the non-linear relationships between the various parameters, to a higher degree. Accurate prediction of core losses can help manufacturers design proper magnetic devices.

The dataset obtained consisted only of field density waveform, frequency, and temperature, and the impact of other notable parameters, if any, are yet to be studied. Also, the model has not been tested for field density waveforms having a considerable DC bias, which needs to be analysed. Alongside these, various types of model architectures and data preprocessing techniques need to be developed and then compared to find the most optimal and accurate ones.

AUTHOR CONTRIBUTIONS

Dixant Sapkota: Conceptualization; data curation; methodology; validation; writing—original draft. **Puskar Neupane:** Formal analysis; investigation; validation; writing—original draft. **Mecon Joshi:** Conceptualization; data curation; validation; writing—original draft. **Shahabuddin Khan:** Supervision; validation; resources.

ACKNOWLEDGEMENTS

The authors would like to thank the organizing team of MagNet challenge 2023 since this research was done as a part of the competition.


CONFLICT OF INTEREST STATEMENT

The authors declare no conflicts of interest.

DATA AVAILABILITY STATEMENT

Data derived from public domain resources. These data were derived from the following resources available in the public domain: Magnet Challenge 2023 Database URL: <https://mag-net.princeton.edu/>

ORCID

Dixant Bikal Sapkota  <https://orcid.org/0009-0007-6025-3586>

Puskar Neupane  <https://orcid.org/0000-0001-7030-7583>

Mecon Joshi  <https://orcid.org/0009-0007-5922-952X>

REFERENCES

- Snelling, E.C.: Soft Ferrites Properties and Applications. Butterworth & Amp; Co, London (1988)
- Muhlethaler, J., Biela, J., Kolar, J.W., Ecklebe, A.: Core losses under the DC bias condition based on Steinmetz parameters. *IEEE Trans. Power Electron.* 27(2), 953–963 (2012)
- Reinert, J., Brockmeyer, A., De Doncker, R.W.: Calculation of losses in ferro- and ferrimagnetic materials based on the modified Steinmetz equation. *IEEE Trans. Ind. Appl.* 37(4), 1055–1061 (2001)
- Albach, M., Durbaum, T., Brockmeyer, A.: Calculating core losses in transformers for arbitrary magnetizing currents a comparison of different approaches. In: *PESC Record. 27th Annual IEEE Power Electronics Specialists Conference*, vol. 2, pp. 1463–1468. IEEE, Piscataway, NJ (1996)
- Li, J., Abdallah, T., Sullivan, C.R.: Improved calculation of core loss with nonsinusoidal waveforms. In: *Conference Record of the 2001 IEEE Industry Applications Conference. 36th IAS Annual Meeting (Cat. No.01CH37248)*, vol. 4, pp. 2203–2210. IEEE, Piscataway, NJ (2001)
- Venkatachalam, K., Sullivan, C.R., Abdallah, T., Tacca, H.: Accurate prediction of ferrite core loss with nonsinusoidal waveforms using only Steinmetz parameters. In: *2002 IEEE Workshop on Computers in Power Electronics, 2002. Proceedings*, pp. 36–41. IEEE, Piscataway, NJ (2002)
- Li, Z., Han, W., Xin, Z., Liu, Q., Chen, J., Loh, P.C.: A review of magnetic core materials, core loss modeling and measurements in high-power high-frequency transformers. *CPSS Trans. Power Electron. Appl.* 7(4), 359–373 (2022)
- Muhlethaler, J., Biela, J., Kolar, J.W., Ecklebe, A.: Improved core-loss calculation for magnetic components employed in power electronic systems. *IEEE Trans. Power Electron.* 27(2), 964–973 (2012)
- Shen, X., Wouters, H., Martinez, W.: Deep neural network for magnetic core loss estimation using the magnet experimental database. In: *2022 24th European Conference on Power Electronics and Applications (EPE'22 ECCE Europe)*, pp. 1–8. IEEE, Piscataway, NJ (2022)
- Serrano, D., Li, H., Wang, S., Guillod, T., Luo, M., Bansal, V., et al.: Why MagNet: quantifying the complexity of modeling power magnetic material characteristics. *IEEE Trans. Power Electron.* 38(11), 14292–14316 (2023)
- Li, H., Serrano, D., Guillod, T., Wang, S., Dogariu, E., Nadler, A., et al.: How MagNet: machine learning framework for modeling power magnetic material characteristics. *IEEE Trans. Power Electron.* 38(12), 15829–15853 (2023)
- Li, H., Serrano, D., Wang, S., Chen, M.: MagNet-AI: neural network as datasheet for magnetics modeling and material recommendation. *IEEE Trans. Power Electron.* 38(12), 15854–15869 (2023)
- Lin, D., Zhou, P., Fu, W.N., Badics, Z., Cendes, Z.J.: A dynamic core loss model for soft ferromagnetic and power ferrite materials in transient finite element analysis. *IEEE Trans. Magn.* 40(2), 1318–1321 (2004)
- LeCun, Y., Bengio, Y., Hinton, G.: Deep learning. *Nature* 521(7553), 436–444 (2015). <https://doi.org/10.1038/nature14539>
- Williams, R.J., Zipser, D.: A learning algorithm for continually running fully recurrent neural networks. *Neural Comput.* 1, 270–280 (1989). <https://api.semanticscholar.org/CorpusID:14711886>
- Anns, A., Jannis, D., Verbeeck, J.: Deep learning for automated materials characterisation in core-loss electron energy loss spectroscopy. *Sci. Rep.* 13(1), 13724 (2023)
- Hochreiter, S., Schmidhuber, J.: Long short-term memory. *Neural Comput.* 9, 1735–1780 (1997)
- Gers, F., Schraudolph, N., Schmidhuber, J.: Learning precise timing with LSTM recurrent networks. *J. Mach. Learn. Res.* 3, 115–143 (2002)
- Staudemeyer, R.C., Morris, E.R.: Understanding LSTM - a tutorial into long short-term memory recurrent neural networks. *arXiv:1909.09586* (2019)
- Zhao, S., Blaabjerg, F., Wang, H.: An overview of artificial intelligence applications for power electronics. *IEEE Trans. Power Electron.* 36(4), 4633–4658 (2021)
- Lin, L., Zhang, J., Gao, X., Shi, J., Chen, C., Huang, N.: Power fingerprint identification based on the improved V-I trajectory with color encoding

- and transferred CBAM-ResNet. PLOS ONE 18(2), 1–23 (2023). <https://doi.org/10.1371/journal.pone.0281482>
22. Serrano, D., Li, H., Guillod, T., Wang, S., Luo, M., Sullivan, C.R., et al.: Neural network as datasheet: modeling B-H loops of power magnetics with sequence-to-sequence LSTM encoder-decoder architecture. In: 2022 IEEE 23rd Workshop on Control and Modeling for Power Electronics (COMPEL), pp. 1–8. IEEE, Piscataway, NJ (2022)
 23. Shen, X., Wouters, H., Martinez, W.: Deep neural network for magnetic core loss estimation using the magnet experimental database. In: 2022 24th European Conference on Power Electronics and Applications (EPE'22 ECCE Europe), pp. 1–8. IEEE, Piscataway, NJ (2022)
 24. Li, H., Serrano, D., Wang, S., Guillod, T., Luo, M., Chen, M.: Predicting the B-H loops of power magnetics with transformer-based encoder-projector-decoder neural network architecture. In: 2023 IEEE Applied Power Electronics Conference and Exposition (APEC), pp. 1543–1550. IEEE, Piscataway, NJ (2023)
 25. Misir, O., Akar, M.: Efficiency and core loss map estimation with machine learning based multivariate polynomial regression model. Mathematics 10(19), 3691 (2022)
 26. Dogariu, E., Li, H., Serrano López, D., Wang, S., Luo, M., Chen, M.: Transfer learning methods for magnetic core loss modeling. In: 2021 IEEE 22nd Workshop on Control and Modelling of Power Electronics (COMPEL), pp. 1–6. IEEE, Piscataway, NJ (2021)
 27. Shen, X., Wouters, H., Martinez, W.: Deep neural network for magnetic core loss estimation using the magnet experimental database. In: 2022 24th European Conference on Power Electronics and Applications (EPE'22 ECCE Europe), pp. 1–8. IEEE, Piscataway, NJ (2022)
 28. Carmona, M.A., Gallego, J., Martinez, A.: Method for accurately predicting core losses using deep learning. In: PCIM Europe digital days 2020; International Exhibition and Conference for Power Electronics, Intelligent Motion, Renewable Energy and Energy Management, pp. 1–7. IEEE, Piscataway, NJ (2020)
 29. Khan, A., Ghorbanian, V., Lowther, D.: Deep learning for magnetic field estimation. IEEE Trans. Magn. 55(6), 1–4 (2019)
 30. Bracewell, R.N., Bracewell, R.N.: The Fourier Transform and its Applications. vol. 31999, McGraw-Hill, New York (1986)
 31. Welch, P.D.: The use of fast fourier transform for the estimation of power spectra: a method based on time averaging over short, modified periodograms. IEEE Trans. Audio Electroacoust. 15, 70–73 (1967)
 32. Ryan, T.J.J.: LSTMs explained: a complete, technically accurate, conceptual guide with keras. Accessed December 5, 2023. <https://medium.com/analytics-vidhya/lstms-explained-a-complete-technically-accurate-conceptual-guide-with-keras-2a650327e8f2> (2020).

How to cite this article: Sapkota, D.B., Neupane, P., Joshi, M., Khan, S.: Deep learning model for enhanced power loss prediction in the frequency domain for magnetic materials. IET Power Electron. 1–12 (2024). <https://doi.org/10.1049/pel2.12704>